Monitoring of the friction stir welding process by means of thermography

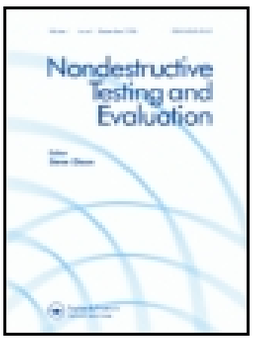

Nondestructive Testing and Evaluation

ISSN: 1058-9759 (Print) 1477-2671 (Online) Journal homepage: http://www.tandfonline.com/loi/gnte20

Monitoring of the friction stir welding process by means of thermography

L.M. Serio, D. Palumbo, U. Galietti, L.A.C. De Filippis & A.D. Ludovico

To cite this article: L.M. Serio, D. Palumbo, U. Galietti, L.A.C. De Filippis & A.D. Ludovico (2016): Monitoring of the friction stir welding process by means of thermography, Nondestructive Testing and Evaluation, DOI: 10.1080/10589759.2015.1121266

To link to this article: http://dx.doi.org/10.1080/10589759.2015.1121266

Published online: 22 Jan 2016.

NONDESTRUCTIVE TESTING AND EVALUATION, 2016
http://dx.doi.org/10.1080/10589759.2015.1121266

Taylor & Francis
Taylor & Francis Group

Monitoring of the friction stir welding process by means of thermography

L.M. Serio, D. Palumbo, U. Galietti, L.A.C. De Filippis and A.D. Ludovico

Department of Mechanics, Mathematics and Management (DMMM), Bari, Italy

ABSTRACT

This work is a study of the thermal behaviour of aluminium alloy 5754-H111 sheets welded with the friction stir welding (FSW) process. In particular, the feasibility of infrared thermography for monitoring of the FSW process is presented. This process has different advantages compared to those of traditional welding, such as very low welding temperature and low mechanical distortion. Usually in the literature, destructive tests are carried out to evaluate the quality of joints, but this approach is time-consuming and off-line. Results have shown that the thermal behaviour of joints is correlated to process parameters and that thermography can be used to perform the online monitoring of the FSW process.

ARTICLE HISTORY
Received 8 September 2015
Accepted 9 November 2015

KEYWORDS
Thermography; process control; monitoring; friction stir welding (FSW); aluminium alloy

1. Introduction

Friction stir welding (FSW) is an innovative joining process, based on the frictional and stirring phenomena, patented at The Welding Institute in 1991.[1] FSW uses a rotating (non-consumable) cylindrical tool that consists of a shoulder and a probe (Figure 1). Welding heat, therefore, is produced by the tool: the shoulder is pressed against the surface of the materials being welded, while the probe is forced between the two components by a downward force; the rotation of the tool generates a frictional heat that decreases the resistance to plastic deformation of the material.[2,3]

The FSW process offers significant advantages when compared with fusion joining processes for aluminium due to a very low welding temperature; mechanical distortion is practically eliminated, with minimal heat affected zone, and there is an excellent surface finish.[2]

For all these reasons, the FSW process is used in the transport industry, in particular in the shipbuilding industry which employs very high corrosion strength alloys such as non-heat-treatable aluminium–magnesium (Al–Mg) alloys (5xxx series). However, in the literature, this process has been less explored as regards aluminium–magnesium (Al–Mg) alloys. In particular, the strong influence of process parameters on the quality of joints has been demonstrated in terms of tensile strength, fatigue behaviour and residual stress.

CONTACT D. Palumbo davide.palumbo@poliba.it

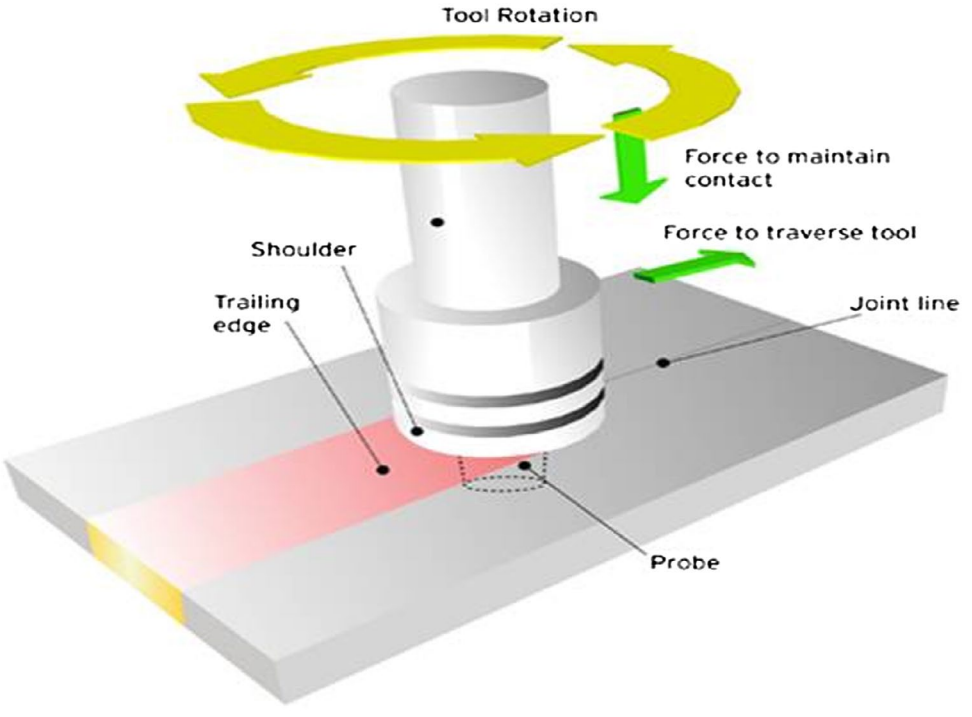

Figure 1. Schematic illustration of FSW butt joint.

Senkara and Zhang [4] and by Miles et al. [5] have documented in detail the behaviour of the AA 5xxx alloys welded with the FSW process and found that the mechanical properties of the joints depend mainly on the grain size and the dislocation density due to the phenomena of plastic deformation and recrystallisation.

Peel et al. [6] analysed the microstructure, the mechanical properties and the residual stresses of friction stir welds of aluminium alloy AA5083 while Kwon et al. [7] studied the application of the friction stir welding to 5052 aluminium alloy plates.

Jin et al. [8] studied the friction stir welding of Al 5754 alloys using constant FSW parameters, and they also have examined the microstructural development and micro hardness distribution in the welds. Attallah et al. [9] conducted a study on the FSW of 2XXX and 5XXX series sheet materials in various tempers at different FSW parameters. These analyses have highlighted the relationship between the banding of constituent particles and "onion rings" formation in the Al 5754 joint.

In the work of Kulekci et al. [10], the effects of the tool pin diameter and tool rotation speed at a constant weld speed were investigated on fatigue properties of friction stir overlap welded alloy Al 5754. Two other works [11,12] provide information on the influence of process parameters, on the tensile and the fatigue behaviour of a friction stir welded joint under a single FSW parameter in a tailor-welded blank of alloy Al 5754. However, the welding parameters were not disclosed by the authors.

In the above-mentioned works, mechanical tests and destructive tests are used to evaluate the quality of joints such as micrographs and macrographs or X-ray diffraction used to measure residual stress.[6–13] These techniques cannot provide information about the

performance of process during welding and require high test times, making them unfeasible for the industrial field.

In this work, the thermographic technique is proposed, directly in production line, to control the FSW process used to weld 6-mm-thick sheets of 5754 H111 aluminium alloy.

Thermography is a full-field contactless technique used for non-destructive evaluation of defects in a wide range of materials and for process monitoring.[14–17] In this work, a passive infrared thermography set-up [13,14] is used to study the thermal behaviour of joints. This approach has been used in the literature for other types of welding.

In the work of Palumbo and Galietti [18], thermal methods were used to study the fatigue behaviour of steel welded joints. In particular, a new procedure has been proposed for monitoring the welded structure during the service condition and to estimate the fatigue limit of material. Sreedhar et al. [19] proposed an automatic online defect detection monitoring aluminium alloy 2219 plates TIG welded in a rotating fixture in order to reduce the time needed for post-weld inspection with X-ray technique.

With regard to FSW process, there are only few studies about the thermal monitoring of FSW process.

Hwang et al. [20] carried out an experimental study of temperature distributions within the work piece during friction stir welding of aluminium alloys while Zhu and Chao [21] performed a numerical simulation of transient temperature and residual stresses in FSW process of 304L stainless steel; Chao et al. [22] assessed the heat transfer in friction stir welding both experimentally and numerically, and Schmidt et al. [23] developed an analytical model for heat generation in FSW.

All these works show applications based only on the measurement of absolute temperature of welded joints during the process with infrared cameras or thermocouples. However, the absolute temperature is affected by environmental conditions and is influenced by experimental set-up adopted for the tests, and subsequently, it cannot be used as a representative parameter of the FSW process.[13]

Therefore, in this work, a more sensitive thermal parameter is proposed for the monitoring of the FSW process. This parameter is representative of the heat generated during the process and, moreover, of the heat rate which is strictly correlated to process parameters.

2. Experimental procedure

The welded specimens for this study were produced by FSW with 5754Al alloy sheets in the H111 condition. The plates have the following dimensions: $L \times W \times H = 200 \times 100 \times 6$ mm and they were butt welded for a length of 170 mm longitudinally to the rolling direction.

The chemical compositions and main mechanical properties of the AA 5754 H111 alloy are, respectively, presented in Tables 1 and 2.

The behaviour of the welds was studied in two combinations of the process parameters. The considered values of the tool rotation speed and the welding speed were, respectively, 500, 700 RPM and 20, 30 cm/min. These parameters were used to construct a 2^2 full factorial experimental plan (Figure 2) with *n*. 2 replications for each combination.

Each test was denominated in accordance with the parameter combination of tool rotation speed (n) and welding speed (v). For example, the indication "R1T1" refers to the replication *n*. 1 and test *n*. 1.

Table 1. Chemical composition of the alloy AA 5754 H111.

	Si	Fe	Cu	Mn	Mg	Cr	Ni	Zn	Ti	Other elements
AA5754-H111	0.40	0.40	0.10	0.50	2.60–3.60	0.30	0.05	0.20	0.15	0.05

Table 2. Mechanical properties of AA 5754 H111 perpendicular to the rolling direction.

	Rm (MPa)	Rp (0.2) (MPa)	HB	*E* [MPa]	Density [g/cm^3]	Thermal conductivity [W/m°C]	Specific heat [Cal/kg°C]
AA5754-H111	190	80	52	70.000	2.65 at room temperature	138 at room temperature	0.213 at room temperature

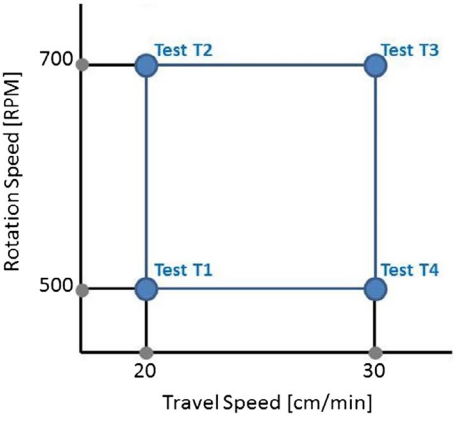

Figure 2. Full factorial plane 2^2 used for experimental tests.

All single-pass friction stir butt welds were made using an FSW tool made of high-strength steel. The tool has a shoulder with a diameter of 22 mm, on which groves were milled to improve the extrusion action on the surface material of the joints, while the tool probe is threaded and truncated. The tool was inclined at 1°, 2° compared to the normal inclination of the workpiece to facilitate mixing of the material.

All welds were carried out in control position using ESAB LEGIO which was equipped with the FSW welding head.

The workpiece was fixed on a rigid backing-plate, and clamped along the welding direction on both sides to avoid lateral movement during welding. The end part of the workpiece was positioned on the worktables as shown in Figure 3.

The thermal acquisitions were performed using two thermal cameras. In particular, in order to acquire the thermal data along the weld tool direction, the cooled FLIR X6540 SC IR camera was used. This latter has thermal sensitivity (NETD) <20 mK and is based on a InSb photonic detector with 640 × 512 pixels. The uncooled FLIR SC640 IR camera (thermal sensitivity (NETD) <30 mK, 640 × 480 pixels) was placed in perpendicular direction compared to the first thermal camera. Sequences were recorded during each test captured at 15 Hz.

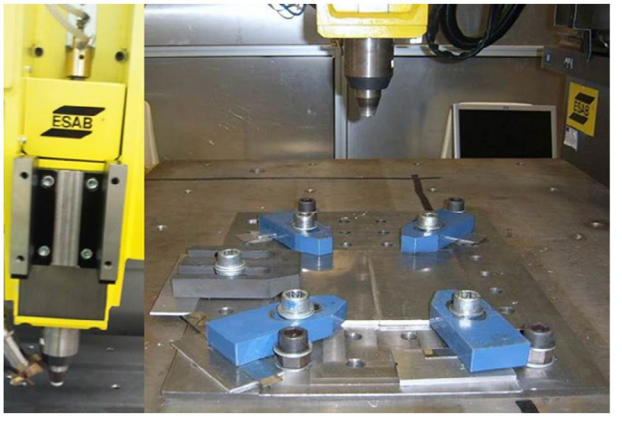

Figure 3. Positioning of the workpiece on the fixture table.

Both thermal cameras recorded the maps of surface temperature, across the weld, for each combination of process parameters as in the experimental plan described and shown in Figure 2. The thermal camera set-up is shown in Figure 4.

Before the tests, specimens were painted with matt black paint (as shown in Figure 5(b)) to provide uniformity of the emissivity of treated surfaces and to avoid reflections caused by heat sources placed near the specimens during the tests.

Temperatures inside the workpiece were measured by twelve N-type thermocouples with a sheath diameter of 1 mm. A digital thermometer was used to acquire the thermocouples data with a sampling frequency of 2 Hz.

To fix the thermocouples in the workpiece, they were set on the surface of the work plates inside twelve small holes with a diameter of about 1 mm according to the layout shown in Figure 5(a).

Three cross sections were chosen to be monitored: Section A, in correspondence with the welding start point, Section B, located in the central area of the weld (generally this section

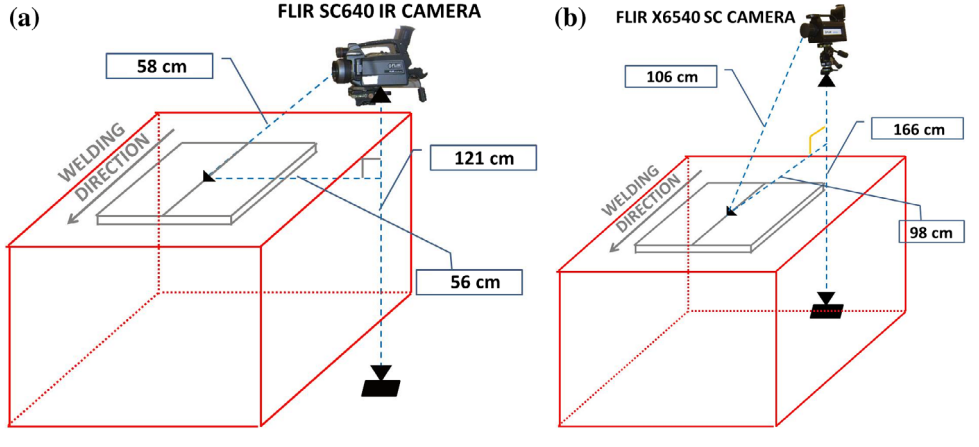

Figure 4. Set-up used for thermographic data acquisition. FLIR X6540 sc IR camera placed along the welding tool direction (a) and Flir sc 640 IR camera placed perpendicular as to the welding tool direction (b).

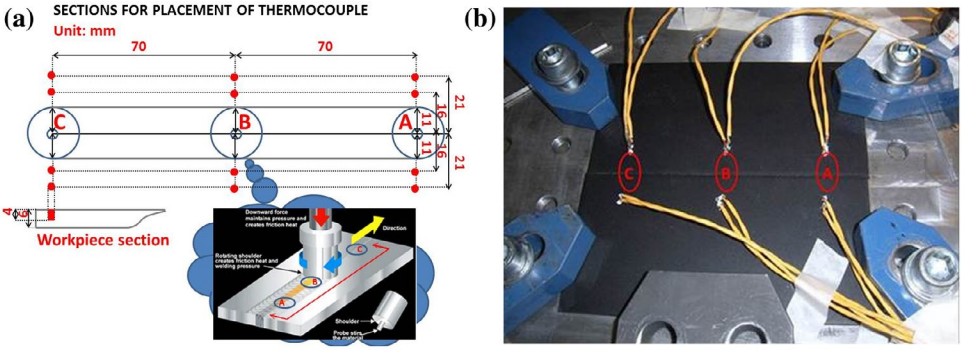

Figure 5. Thermocouples layout (a) and workpiece set-up (b).

is considered to be over the transient due to the penetration of the tool into the workpiece) and Section C, in correspondence with the end of the welding and the extraction of the tool. For each section, four thermocouples were placed, respectively, two on the advancing side and two on the retreating side. On each side, the thermocouples are positioned at different distances from the centre of the welding line in order to obtain temperature information at different distances from the weld central area (nugget).

3. Results and discussion

3.1. Thermal behaviour

Thermal acquisitions provided very important information about the FSW process. As a rule:

- During the tests, a thermal asymmetry of the joints is evident, due to the various orientations of the speed vectors which came into play during the process. This occurred for each combination of process parameters.
- The results showed for each test that the temperatures in the retreating side of welds are higher than on the advancing side as shown in Figure 6. In particular, the maximum temperatures measured were reported with thermocouples in correspondence

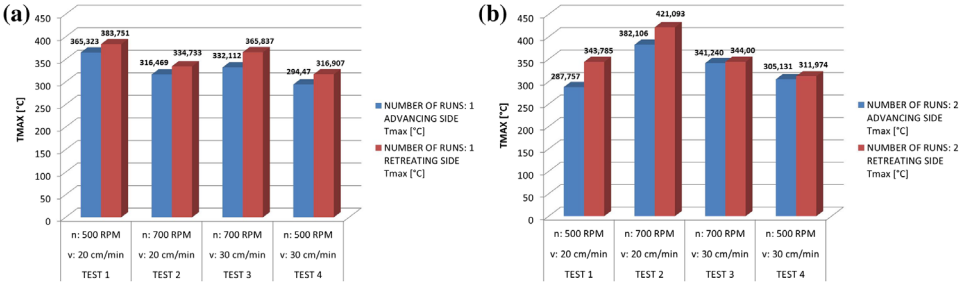

Figure 6. Histogram of the maximum temperatures recorded along the advancing and retreating side for all the tests of the experimental plan. Tmax recorded during the first replication (a) and Tmax recorded during the second replication (b).

of Section B (distance 5 mm) for the first replication (Figure 6(a)) and the second replication (Figure 6(b)).

- Significant differences can be observed between the maximum temperatures measured in the 1st and 2nd replications. These are due to the high temperature gradient (Figure 6) in the area in which thermocouples were placed. Then, a minimum error in relative positioning between weld and thermocouple can give the measured difference of the temperature.

Temperatures measured with thermocouples in the Section A, B and C (Figure 5(a)) show a non-uniform temperature trend along the weld. For example, Figure 8 shows the thermal profiles registered by the thermocouples placed on advancing and retreating side in correspondence with Sections A, B and C.

In Figure 8, three thermal profiles are shown, obtained by thermographic sequences in correspondence with the thermocouples placed at 21 mm from the centre of weld (test *n*. 1, n = 500 RPM; v = 20 cm/min). Thermographic temperature data on the surface of the aluminium plates show similar thermal trends compared with thermocouple data (Figure 7).

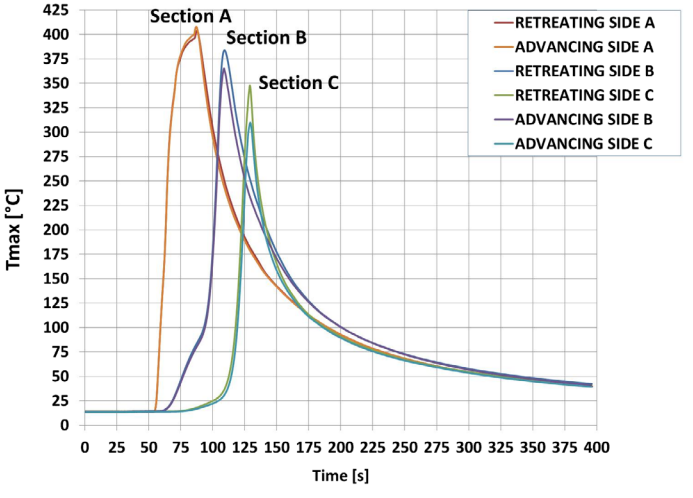

Figure 7. Thermal profiles on the advancing and retreating side acquired by thermocouples placed at 21 mm from the central line of joint (test *n*. 1, n = 500 RPM; v = 20 cm/min) in correspondence with three sections of the welding.

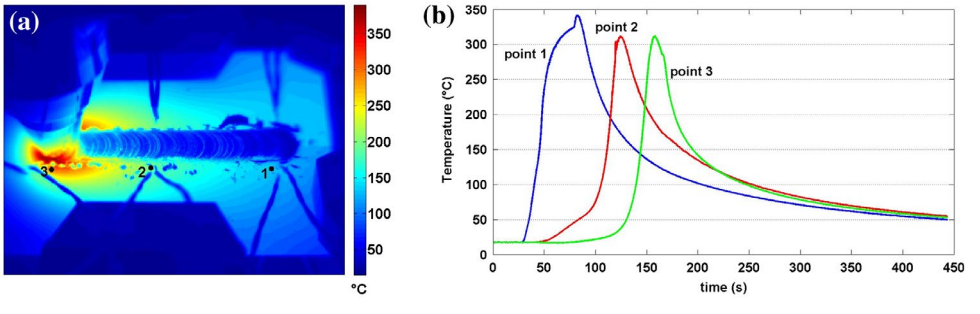

Figure 8. (a) Image obtained at the end of the welding process, (b) thermal profiles obtained over time by thermographic sequences in correspondence with Sections A, B and C (test 1).

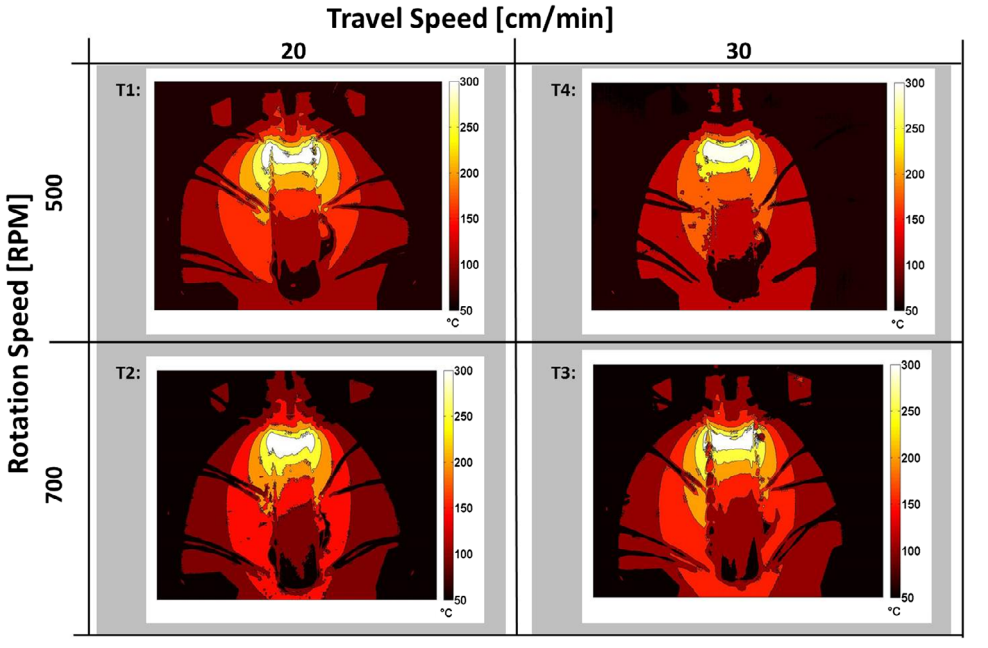

Figure 9. Thermal maps obtained during the tests in a fixed time instant: Test 1: $v = 20$ [cm/min] – $n = 500$ [RPM]; Test 2: $v = 30$ [cm/min] – $n = 700$ [RPM]; Test 3: $v = 20$ [cm/min] – $n = 700$ [RPM]; Test 4: $v = 30$ [cm/min] – $n = 500$ [RPM].

These results were also confirmed by the thermographic maps (Figure 9) acquired for each test and referred to a given instant time.

Thermographic data allow us to obtain a full field of information on the temperatures reached during the tests and so could replace thermocouples generally used in the literature to measure the temperature during an FSW process.

Despite the presence of the paint could theoretically influence the behaviour of the joint, no evidence of increased presence of defects was found on the basis on macrography.[13] Moreover, the aim of the work was to set a possible set-up for monitoring the process, and in this work, authors demonstrated this possibility performing the analysis on the side of the welding itself. The final procedure forecast no painting on the area interested by the welding.

Other thermal data can be used to monitor the FSW process with higher efficiency. For example, the maximum temperature (Tmax), reached during the weld process, is generally linked to process parameters and then it could be correlated with the mechanical and structural properties of welded joints.

In order to evaluate the Tmax reached during the welding process, the thermal sequences acquired for each test were analysed with Matlab™ software. Figure 10 shows the Tmax maps obtained analysing the sequences of second replication, recorded with the Flirsc 640 thermal camera. These maps represent the maximum temperature reached by each pixel during the test independently of time.[15]

The results were in agreement with the thermocouple data. In fact, each test shows a non-uniform distribution of Tmax along the welding direction. These maps confirm that the stationary conditions of the welding process along the joints have not yet been reached.

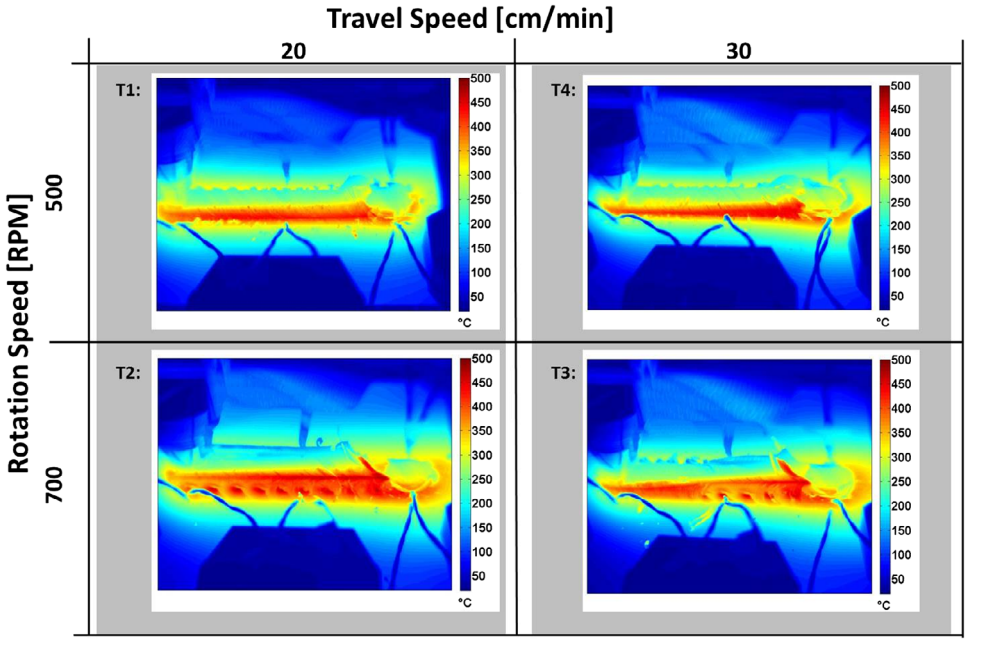

Figure 10. Maps of Tmax assessed for each test: Test 1: $v = 20$ [cm/min] – $n = 500$ [RPM]; Test 2: $v = 30$ [cm/min] – $n = 700$ [RPM]; Test 3: $v = 20$ [cm/min] – $n = 700$ [RPM]; Test 4: $v = 30$ [cm/min] – $n = 500$ [RPM].

A quantitative evaluation of Tmax maps can be performed considering thermal profiles at different distances from Section A. In particular, Figure 11(a) reports a thermal profile obtained along the y axis and the best fit of data obtained with a cubic equation (test R1T3). This equation could allow us to estimate the temperature along the y direction as documented in the study of Hwang et al. [20].

However, it was not possible to use the best fit equation to assess the Tmax at the centre of joint ($y = 0$) or generally in the weld area due to the complicated thermal phenomena that occurred in this area.

Moreover, Tmax was assessed along the joint, as shown in Figure 11(b), at the distance of 21 mm from the central line of the welded joint. It was clearly evident that the Tmax decreased along the weld due to the non-stationary condition of the weld process.

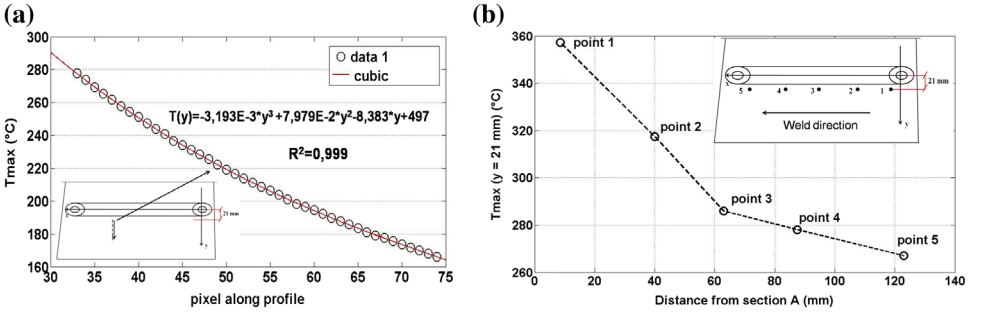

Figure 11. Thermal profile along the y axis and the best fit of data obtained with a cubic equation (a), Tmax trend along the weld direction (b).

The different values of Tmax are probably correlated with different structural and mechanical properties of the joint along the weld direction. However, measurements of absolute temperatures are affected by environmental conditions and are highly influenced by the specific set-up used for the tests. Therefore, it is difficult to correlate the Tmax values with the process parameters.

A likely and more sensitive thermal parameter is the heat rate, as directly correlated with the energy and then the heat supplied during the welding process. This parameter is proportional to the slope of heating curve obtained for a defined point considered on the surface of joints. In this case, the slope of heating curve is evaluated in two sections of work piece and on the retreating side and advanced side (Figure 12) in order to obtain a total of 4 values for each test.

The considered points are positioned to 120 mm (a1 and a2 in Figure 12) and to 20 mm (b1 and b2) from the start of welding, which is characterised by the transience phase of the process due to the penetration of the tool. In particular, for each thermal profile of each point, the maximum slope of heating curve is evaluated (MSHC), (Figure 12(b)).

The values of maximum slope were evaluated through the processing of thermographic data. In particular, the linear best fit on 70 temperature data of each profile (Figure 12(b)) was used to assess the maximum slope value (Figure 13). In Figure 13, the different heating slope obtained at different positions from the start of welding is clearly evident, while there seems to be no difference between retreating and advancing sides.

Table 3 shows the MSHC values assessed for each test expressed in terms of angular measurement (degrees) compared to the horizontal axis.

3.2. Statistical analysis of thermal results

The thermal parameter MSHC can be used for the monitoring of the FSW process if it is correlated to process parameters. Therefore, a statistical analysis (ANOVA) has been

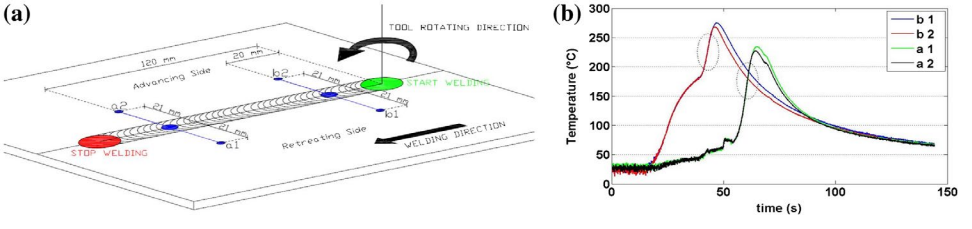

Figure 12. (a) Positioning of the measurement points along the welding line, used for the analysis of MSHC, (b) thermal profile obtained for the points a1, a2, b1 and b2 (test R1T3).

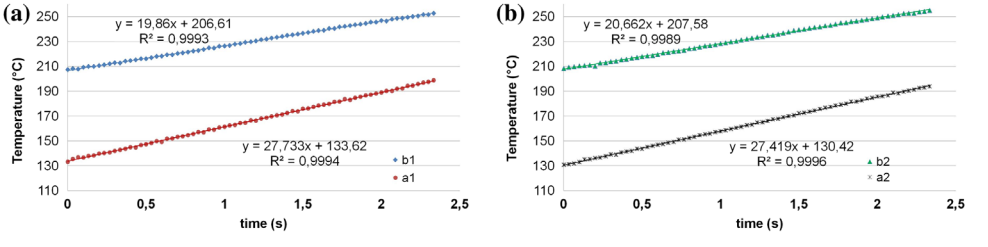

Figure 13. Evaluation of heating slope in points a1, b1 and a2, b2: comparison on (a) R.S. and (b) A.S., test R1T3.

Table 3. Values of MSHC for each test.

		Travel speed [cm/min]			
		20		30	
Rotation speed [RPM]	500	R1T1	R2T1	R1T4	R2T4
		a1: MSHC: 87,246°	a1: MSHC: 87,587°	a1: MSHC: 87,968°	a1: MSHC: 87,575°
		a2: MSHC: 86,800°	a2: MSHC: 87,433°	a2: MSHC: 87,911°	a2: MSHC: 88,448°
		b1: MSHC: 86,051°	b1: MSHC: 86,596°	b1: MSHC: 89,066°	b1: MSHC: 86,883°
		b2: MSHC: 85,825°	b2: MSHC: 86,161°	b2: MSHC: 86,846°	b2: MSHC: 87,229°
	700	R1T2	R2T2	R1T3	R2T3
		a1: MSHC: 87,229°	a1: MSHC: 87,480°	a1: MSHC: 88,140°	a1: MSHC: 88,530°
		a2: MSHC: 87,911°	a2: MSHC: 87,735°	a2: MSHC: 88,146°	a2: MSHC: 88,319°
		b1: MSHC: 87,117°	b1: MSHC: 86,528°	b1: MSHC: 87,371°	b1: MSHC: 87,735°
		b2: MSHC: 87,921°	b2: MSHC: 87,998°	b2: MSHC: 87,371°	b2: MSHC: 88,228°

Table 4. General linear model: heating slope vs. travel speed; rotation speed; position samples along the welding direction and side of the welding.

Term	Effect	Coef	SE Coef	*T*	*P*-value
Constant		87.4808	0.08715	1003.78	0.000
v	0.7592	0.3796	0.08715	**4.36**	**0.000**
n	0.5084	0.2542	0.08715	**2.92**	**0.010**
p	0.5957	0.2979	0.08715	**3.42**	**0.004**
Side	0.0737	0.0369	0.08715	0.42	0.678
$v \times n$	−0.2691	−0.1346	0.08715	−1.54	0.142
$v \times p$	−0.0572	−0.0286	0.08715	−0.33	0.747
$v \times$ side	−0.1700	−0.0850	0.08715	−0.98	0.344
$n \times p$	−0.1931	−0.0966	0.08715	−1.11	0.284
$n \times$ side	0.3636	0.1818	0.08715	2.09	0.053
$P \times$ side	0.0447	0.0224	0.08715	0.26	0.801
$v \times n \times p$	0.2621	0.1311	0.08715	1.50	0.152
$v \times n \times$ side	−0.1954	−0.0977	0.08715	−1.12	0.279
$v \times p \times$ side	0.2042	0.1021	0.08715	1.17	0.258
$n \times p \times$ side	−0.2991	−0.1496	0.08715	−1.72	0.105
$v \times n \times p \times$ side	−0.1244	−0.0622	0.08715	−0.71	0.486

Significance level: 0.05.
$S = 0.493004$. R-Sq = 78.01%. R-Sq(adj) = 57.40%.
The bold values represent the main results of the ANOVA.

carried out in order to verify the statistical significance of the effect produced by process parameters on MSHC.

A 2^4 full factorial experimental plan has been carried out, considering the maximum heating slope value – MSHC (Table 3) as response variable and the rotation speed, the travel speed, the position of specimen along the welds and the side of the welding as factors.

Statistical analysis, performed with the MINITAB™ software, showed that the maximum heating slope is influenced by the rotation speed, the position of the specimens along the welding and the travel speed. The main results of this analysis are summarised in Table 4.

An empirical model can be obtained in order to correlate all the significant parameters. Performing a regression analysis, the following model is obtained:

$$\mathrm{MSHC} = 83,558 + 0.0722v + 0.002668n + 0.00688p \quad (1)$$

The analysis of ANOVA showed that the parameter MSHC is influenced both on tool rotation speed (n) and welding speed (v). The dependence on position p is due to the non-stationary condition of process. Therefore, thermography could be used for online monitoring of the FSW process by means of a thermal parameter (MSHC) correlated with the process parameters.

4. Conclusions

This work studies the thermal behaviour of 5754-H111 plates joined by friction stir welding. In particular, a new thermographic procedure is proposed for online monitoring of process. The main considerations could be summarised as follows:

- Thermal data acquired with both thermocouples and thermal cameras show an evident non-symmetrical FSW process in terms of temperatures measured during the tests. Moreover, the higher temperatures were measured along the retreating side for each parameter combination.
- Thermal data analysis shows a non-stationary welding process. In particular, the maximum temperature was evaluated for each test and a non-uniform trend of Tmax was obtained along the welding direction.
- Thermographic technique can be a powerful tool for monitoring of the FSW process through the measurement of surface temperatures on welded joints. In particular, through very easy analysis, the stationary quality of the FSW process could be assessed in terms of the maximum temperatures reached during the process.
- The feasibility of infrared thermography for monitoring of the FSW process is shown. In particular, in non-stationary conditions, the maximum heating slope of thermal profiles evaluated on surface of joints can be used for monitoring the process parameters.

Disclosure statement

No potential conflict of interest was reported by the authors.

References

[1] W.M.Thomas, E.D.Nicholas, J.C.Needham, M.G.Murch, P.Temple-Smith, C.J.Dawes. Friction Stir Butt Welding. International Patent Application No. PCT/GB92/02203 and GB Patent Application No. 9125978.8 and US Patent Application No. 5,460,317, December 1991.
[2] Nandan R, Debroy T, Bhadeshia HKDH. Recent advances in friction-stir welding – process, weldment structure and properties. Prog. Mater. Sci. 2008;53:980–1023.
[3] Rodrigues DM, Leitão C, Louro R, et al. High speed friction stir welding of aluminium alloys. Sci. Technol. Weld. Joining. 2010;15:676–681.
[4] Senkara J, Zhang H. Cracking in spot welding aluminium alloy AA5754. Weld. J. 2000;79:194–201.
[5] Miles MP, Nelson TW, Decker BJ. Formability and strength of friction-stir-welded aluminum sheets. Metall. Mater. Trans. A. 2004;35:3461–3468.
[6] Peel M, Steuwer A, Preuss M, et al. Microstructure, mechanical properties and residual stresses as a function of welding speed in aluminium AA5083 friction stir welds. Acta Mater. 2003;51:4791–4801.

[7] Kwon YJ, Shim SB, Park DH. Friction stir welding of 5052 aluminum alloy plates. Trans. Nonferrous Met. Soc. China. 2009;19:s23–s27.
[8] Jin H, Saimoto S, Ball M, et al. Characterisation of microstructure and texture in friction stir welded joints of 5754 and 5182 aluminium alloy sheets. Mater. Sci. Technol. 2001;17:1605–1614.
[9] Attallah MM, Davis CL, Strangwood M. Influence of base metal microstructure on microstructural development in aluminium based alloy friction stir welds. Sci. Technol. Weld. Joining. 2007;12:361–369.
[10] Kulekci M, Şik AS, Kaluç E. Effects of tool rotation and pin diameter on fatigue properties of friction stir welded lap joints. Int. J. Adv. Manuf. Technol. 2008;36:877–882.
[11] Barlas Z, Ozsarac U. Effects of FSW parameters on joint properties of Al Mg3 alloy. Weld. Res. 2012;91:16-s.
[12] Garware M, Kridli GT, Mallick PK. Tensile and fatigue behaviour of friction-stir welded tailor-welded blank of aluminum alloy 5754. J. Mater. Eng. Perform. 2010. doi:10.1007/s11665-009-9589-1.
[13] Serio LM, Palumbo D, Galietti U, et al. Analisi del processo di Friction Stir Welding applicato alla lega AA 5754 H111: comportamento meccanico e termico dei giunti. Rivista Italiana della Saldatura. 2014.
[14] Maldague XPV. Theory and practice of infrared technology of non-destructive testing. New York, NY: Wiley; 2001;19:1161–1171.
[15] Palumbo D, Ancona F, Galietti U. Quantitative damage evaluation of composite materials with microwave thermographic technique: feasibility and new data analysis. Meccanica. 2014;50:443–459.
[16] Schlichting J, Brauser S, Pepke LA, et al. Thermographic testing of spot welds. NDT&E Int. 2012;48:23–29.
[17] Galietti U, Cavicchia A, Spagnolo L. Nondestructive control of glass components by means of thermography. In: SPIE Proceedings, Thermosense XXIV. 2002;4710. doi:10.1117/12.459588.
[18] Palumbo D, Galietti U. Characterisation of steel welded joints by infrared thermographic methods. QIRT J. 2014;11:29–42.
[19] Sreedhar U, Krishnamurthy CV, Balasubramaniam K. Automatic defect identification using thermal image analysis for online weld quality monitoring. J. Mater. Process. Technol. 2012;212:1557–1566.
[20] Hwang YM, Kang XW, Chiou YC, et al. Experimental study on temperature distributions within the workpiece during friction stir welding of aluminum alloys. Int. J. Mach. Tools Manuf. 2008;48:778–787.
[21] Zhu XK, Chao YJ. Numerical simulation of transient temperature and residual stresses in friction stir welding of 304L stainless steel. J. Mater. Process. Technol. 2004;146:263–272.
[22] Chao YJ, Qi X, Tang W. Heat transfer in friction stir welding – experimental and numerical studies. J. Manuf. Sci. Eng. 2003;125:138–145.
[23] Schmidt H, Hattel J, Wert J. An analytical model for the heat generation in friction stir welding. Modell. Simul. Mater. Sci. Eng. 2004;12:143–157.